



**HAL**  
open science

## Multititration: The New Method for Implementing Ultrasensitive and Quantitative Multiplexed In-Field Immunoassays Despite Cross-Reactivity?

Fanny Mousseau, Cécile Féraudet Tarrise, Stéphanie Simon, Thierry Gacoin, Antigoni Alexandrou, Cédric Ismael Bouzigues

### ► To cite this version:

Fanny Mousseau, Cécile Féraudet Tarrise, Stéphanie Simon, Thierry Gacoin, Antigoni Alexandrou, et al.. Multititration: The New Method for Implementing Ultrasensitive and Quantitative Multiplexed In-Field Immunoassays Despite Cross-Reactivity?. *Analytical Chemistry*, 2023, 95 (36), pp.13509-13518. 10.1021/acs.analchem.3c01846 . hal-04273892

**HAL Id: hal-04273892**

**<https://hal.science/hal-04273892>**

Submitted on 8 Nov 2023

**HAL** is a multi-disciplinary open access archive for the deposit and dissemination of scientific research documents, whether they are published or not. The documents may come from teaching and research institutions in France or abroad, or from public or private research centers.

L'archive ouverte pluridisciplinaire **HAL**, est destinée au dépôt et à la diffusion de documents scientifiques de niveau recherche, publiés ou non, émanant des établissements d'enseignement et de recherche français ou étrangers, des laboratoires publics ou privés.

# Multi-titration: the new method for implementing ultra-sensitive and quantitative multiplexed in-field immunoassays despite cross-reactivity?

F. Mousseau<sup>a\*</sup>, C. Féraudet Tarrisse<sup>b</sup>, S. Simon<sup>b</sup>, T. Gacoin<sup>c</sup>, A. Alexandrou<sup>a</sup> and C. I. Bouzigues<sup>a</sup>

<sup>a</sup> Laboratoire d'Optique et Biosciences, Ecole Polytechnique, Institut Polytechnique de Paris, CNRS, INSERM, Route de Saclay, 91128 Palaiseau, France.

<sup>b</sup> Université Paris-Saclay, CEA, INRAE, Département Médicaments et Technologies pour la Santé (DMTS), 91191 Gif-sur-Yvette, France.

<sup>c</sup> Laboratoire de Physique de la Matière Condensée, Ecole Polytechnique, Institut Polytechnique de Paris, CNRS, Route de Saclay, 91128 Palaiseau, France

Corresponding author: fanny.mousseau@polytechnique.edu

## Abstract

The accurate on-field titration of multiple pathogens is essential to efficiently describe and monitor environmental or biological contamination, isolate, act and treat adequately. This underscores the requirement of portable, fast, quantitative and multiplexed detection technologies, which however have not been properly developed so far, notably because it has been hindered by the phenomenon of cross-reactivity. In this work, we proposed a new analytical method based on the imaging through a portable device of lanthanide-based nanoparticles (YVO<sub>4</sub>:Eu) for spatially multiplexed detection, relying on a multiparameter analysis, *i.e.* a simultaneous analysis of all the luminescence signals through the comparison to a calibration surface built in the presence of multiple analytes of interest. We then demonstrated the possibility to simultaneously quantify by multiplexed Lateral Flow Assay (xLFA) the three enterotoxins SEG, SEH, and SEI in unknown mixtures, over two concentration decades (from a dozen of pg.mL<sup>-1</sup> to few ng.mL<sup>-1</sup>), with a high the recovery of the nominal concentrations (20%), reliability (cross reactive CV < 30%) and sensitivities (apparent LOBs of 3, 27, and 6 pg.mL<sup>-1</sup> for SEG, SEH, and SEI respectively, and apparent LODs of 6, 48, and 11 pg.mL<sup>-1</sup> for SEG, SEH, and SEI respectively). The results were obtained in less than an hour (25 min of strip migration followed by 30 min of drying at room temperature), time during which the presence of the operator was not required for more than 5 min, in order to dip the strip and have it imaged by the reader. Based on this method, we observed an increase in sensitivity of 100 compared to the other multiplexed LFA labeled with gold particles and we approached the sensitivity of the simplex ELISA performed with the same capture and detection antibodies.

To conclude, our results, which are applicable to virtually any kind of multiplexed test, pave the way to the next generation of in-field analytical immunoassays by providing fast, quantitative and highly sensitive multiplexed detection of biomarkers or pathogens.

## Key words

Multiplexed LFA, cross-reactivity, quantitative analysis, europium-doped luminescent nanoparticles.

## Introduction

The development of powerful and portable analytical methods is critical in many domains like environmental monitoring, food quality control, and medical diagnosis, in order to provide an accurate description of the sample and to elaborate possible prevention or treatment strategies. The implementation of a simultaneous quantitative and sensitive detection of a panel of markers in the same sample and within a single experimental procedure, *i.e.* the implementation of a quantitative multiplexed detection, is thus essential<sup>1,2</sup>. In addition, the World Health Organization (WHO) recently published the ASSURED criteria for point-of-care (POC) devices, specifying their functional requirements (Affordable, Sensitive, Specific, User-friendly, Rapid and robust, Equipment-free and Deliverable to end-users)<sup>3</sup>. The Lateral Flow Assay (LFA), also known as immunochromatographic (strip) test, is the technology that best meets these specifications and is therefore expanding rapidly<sup>4</sup>. Considering these two points, the development of sensitive quantitative multiplex LFAs (xLFAs) is of utmost importance.

LFA is currently the most effective and widely used in-field testing approach, due to its structural simplicity, portability, rapidity (5-30 min), specificity, user-friendly format, and cost-effectiveness<sup>1,2,5</sup>. These wicking-membrane-based devices allow sandwich immunoassays for liquid samples *via* biological recognition between antigen and antibodies. They were mainly developed for the detection of a single analyte per assay (LFAs in simplex format) but their architecture particularly suits spatial multiplexing since it enables the presence of more than one detection area in a single device<sup>1,2,4,6</sup>, as illustrated in Figure 1. Multiplexed LFA is a promising strategy for the next generation of biosensors since it consumes smaller sample volumes, fewer materials, offers higher throughput and requires shorter average

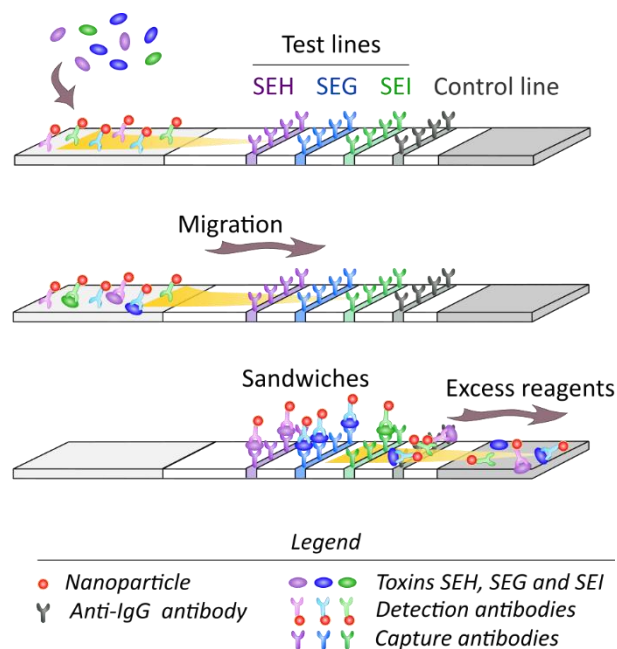


Figure 1: Principle of a multiplexed LFA test for the simultaneous detection of three analytes - When the sample is deposited on the LFA strip, it migrates by capillarity. If the antigen of interest (here toxin) is present, it first interacts with the detection antibodies labeled by a probe (here, our luminescent nanoparticles). The resulting complexes then migrate along the strip and interact with the capture antibodies on the dedicated test lines. Finally, the sample and the particles flow through the control line, which consist of a secondary antibody whose purpose is to capture the remaining probe-labeled antibodies in order to assess the correct running of the assay.

analysis time than individual tests<sup>1,4,7</sup>. However, this technology still faces some limitations. On the one hand, xLFAs cannot detect analytes over a wide range of concentration and do not provide accurate quantitative information<sup>7,8</sup>. On the other hand, they often lose sensitivity compared to the simplex assays. Both these limitations are mainly due to the presence of non-specific binding and cross-reactivity (*i.e.* the ability of antibodies to non-specifically bind other targets in the sample)<sup>9</sup>.

The widespread phenomenon of cross-reactivity has been flagged as one of the biggest obstacle in establishing high performance and large scale multiplexed immunoassays<sup>8-10</sup>. It is highly dependent on the analyte, on the antibodies, on the reporter and on the instrumental settings, and can be responsible for increasing background noise, therefore affecting the assays' limit of detection, generating false positives, and is critical for analyte quantification<sup>7-9,11</sup>. The presence of an additional non-specific signal, either due to reactions between detection reagents, or induced by the analyte, indeed hinders the accurate titration of the target analyte, notably in an unknown complex environment, in which cross-contributions are not *a priori* known and can thus not be considered as a constant non-specific background. Different strategies have thus been developed during the two last decades to mitigate cross-reactivity in multiplexed immunoassays and preserve sensitivity.

Some approaches aim at separating *in situ* the different reagents and/or analytes, either by prior fractionation of the sample<sup>12</sup> which may provide a large-scale multiplexing, or on reagent colocalization followed by an ELISA-like detection. These latter methods eliminate non-specific binding between antibodies and drastically limit analyte induced cross-reactivity by avoiding the mixing of capture and detection antibodies, *e.g.* through a specific spotting on microarrays<sup>13,14</sup>. Another alternative to detect multiple targets in a complex environment is the use of mass spectrometry, which may achieve high sensitivity and selectivity, *e.g.* through the commercial SISCAPA solution<sup>15,16</sup>. However, these methods are complex to implement and require expensive and non-portable equipment, or are not compatible with the LFA technology<sup>8</sup>. An approach to tackle this issue is the development of multicolor LFAs, where each target is revealed by different reporters exhibiting a unique color<sup>4,6,17-25</sup>.

Originally, multicolor LFAs were spatially multiplexed so that each analyte was detected on its own test line, and by a probe whose color was unique, and therefore different from that of the other probes. Although the synthesis of multiple probes complicates the development of the test and increases its cost, the implementation of a multicolor test considerably simplifies the visual control of each target compound for qualitative reading by the naked eye<sup>4,6,18,19</sup>. On the other hand, the number of analytes detected is low because it is limited by the length of the strip. To overcome this problem, two-parameter multiplexing systems based on spatial separation and color colocalization, as illustrated by Zhang *et al.* who detect the simultaneous presence or absence of 5 analytes with the naked eye *via* the use of 2 test lines and 3 different probes<sup>25</sup>.

The use of multicolour tests is also useful for the development of quantitative multiplexed LFAs. However, spectral decomposition of the signal at the level of the test zones is then necessary to reveal the signature of each probe<sup>21</sup>, especially if several analytes are detected on the same test line<sup>4,22,23</sup>. Furthermore, in cases where a test line detects only a single nanoparticle type, the use of multicolored probes in a multiplexed system reduces cross-reactivity but does not eliminate it. In fact, cross-reactivity due to detection antibodies remains unchanged, as illustrated in the following example. Consider a multiplexed assay with two proteins P<sub>1</sub> and P<sub>2</sub>, respectively associated with capture antibodies Ab<sub>C1</sub> and Ab<sub>C2</sub>, and different colored reporters R<sub>1</sub> and

R<sub>2</sub> respectively coupled to detection antibodies Ab<sub>D1</sub> and Ab<sub>D2</sub>. By analytically performing a spectral filtration of the color photos of xLFA tests for which each test line binds only one type of probe, it is possible to eliminate the signal coming from the Ab<sub>C1</sub>-P<sub>1</sub>-Ab<sub>D2</sub>-R<sub>2</sub> or Ab<sub>C1</sub>-P<sub>2</sub>-Ab<sub>D2</sub>-R<sub>2</sub> sandwiches on the test line for recognition of the P1 protein but not those Ab<sub>C1</sub>-P<sub>2</sub>-Ab<sub>D1</sub>-R<sub>1</sub>.

Another solution is the development of highly selective antibodies<sup>7</sup>. Though this can provide cross-reaction reduction in single target tests, no tests for actual quantitative multiplexed assays<sup>17,19</sup> - *i.e.* with multiple targets and detection capabilities – have been reported so far. Indeed, most of the time, in spatial multiplexed assays, only simplex samples are studied on the multiplexed strips for the construction of calibration curves. Furthermore, the development of highly selective antibodies for each protein of interest is time consuming and prevents the rapid development of new multiplexed assays. Despite many efforts, multiplexed determination of protein concentrations with high sensitivity, specificity and accuracy remains a major challenge. Consequently, the failure to adequately account for cross-reactivity in multiplexed immunoassays strongly limits their performances<sup>8</sup> and hinders any quantitative detection<sup>9</sup>. This prevents their efficient use for actual food or environmental monitoring and diagnosis applications.

To circumvent these drawbacks, we here propose to use an integrated new analytical solution for a sensitive quantitative multiplexed immuno-detection, through the imaging of luminescent YVO<sub>4</sub>:Eu nanoparticles by a portable device. As reported in our previous work<sup>26</sup>, aiming at a sensitive detection, we developed the use of new luminescent LFA probes (yttrium vanadate nanoparticles doped with luminescent europium ions) that do not undergo photobleaching or blinking. We have demonstrated that with a simple, affordable and portable home-made UV LED-based reader coupled to a smartphone, we could quantitatively detect different analytes through simplex LFA with a sensitivity enhancement by a factor of 10 to 50 compared to reference LFAs based on gold nanoparticle probes and performed with the same antigen and capture/detection antibody pairs<sup>5</sup>. However, we have shown that, even in a low cross-reactivity regime, the quantitative calibration curves obtained for simplex LFAs with a single analyte did not allow the recovery of the nominal concentration of samples containing multiple analytes<sup>26</sup>.

Here, based on the same system, we develop a strategy to perform multi-titration, *i.e.* quantitative analysis for multiplexed samples even in the presence of non-negligible cross-reactivity<sup>26</sup>. Our new analytical method is based on the establishment of a multiparameter calibration surface, which describes the luminescence responses in the presence of several analytes (*e.g.* proteins) in the sample. Its main feature is that cross-reactivity is no longer an issue for reliable quantification, even in the most unfavourable case, *i.e.* in a high cross-reactivity regime without any additional signal separation. We applied this approach to three enterotoxins, SEG, SEH, and SEI, which are among the 19 different Staphylococcal Enterotoxins (SEs) known to induce staphylococcal food poisoning<sup>27</sup>. Due to their more recent discovery, they have been *de facto* less studied than other SEs although they seem to be similarly harmful<sup>27</sup>. Their rapid and portable detection in food and water matrices has been limited until now, although it is of paramount importance from the point of view of both food safety and protection from biological weapons<sup>28</sup>. Here, we demonstrate the possibility to simultaneously quantify the three toxins, SEG, SEH, and SEI, in a single sample run on a spatial multiplexed strip, with excellent sensitivity and accuracy, *via* a measurement system compatible with in-field analytical immunoassays.

## Material and Methods

### CHEMICALS

All chemical and salts (see the Supplementary Information S1) were used without purification. Deionized water was obtained from a Millipore Milli-Q Water system (Merck). All the buffers were freshly prepared before use.

### MATERIALS

#### *Antibodies and antigens.*

The recombinant toxins SEG ( $M_w = 28.2$  kDa), SEH ( $M_w = 26.3$  kDa) and SEI ( $M_w = 26.1$  kDa) were expressed in *E. coli*, purified, characterized by mass spectrometry, and inoculated to *Biozzi* mice<sup>27,29</sup>. Monoclonal antibodies (Abs) against SEG, SEH and SEI were raised in these mice. They were then produced by hybridomas, purified by protein A affinity chromatography and their biochemical properties were characterized<sup>27</sup>. We invite the reader to consult our previous work for further details<sup>26,27,29</sup>.

#### *Nanoparticles.*

The luminescent nanoparticles (NPs)  $YVO_4:Eu$  (20 %) were synthesized by salt co-precipitation, were chemically surface-modified to allow their covalent coupling to the detection antibodies (targeted Ab:NP molar ratio of 20, *i.e.* 0.01 Ab per  $nm^2$ ), and were characterized by physico-chemical methods, as described in our previous work<sup>15,19</sup> and summarized in S2. Three type of nanoparticles were prepared from the same bare NPs: the  $NP_{SEG}$ ,  $NP_{SEH}$  and  $NP_{SEI}$ , which were coupled to detection antibodies against SEG, SEH, and SEI respectively<sup>30</sup>. A faire par Fanny :Ajouter les propriétés spectrales (surtout illumination dans l'UV)(dans l'intro aussi ?)

### METHODS

#### *Strip assembly.*

All three test lines were printed with capture antibodies (prepared as described in Materials and diluted to  $1 \text{ mg.mL}^{-1}$  in potassium phosphate buffer - 50 mM, pH 7.4) with a Frontline<sup>TM</sup> microliter contact dispenser (BioDot, USA,  $1 \mu\text{L.cm}^{-1}$ , 50  $\text{mm.s}^{-1}$ ) onto a FF120HP nitrocellulose membrane (Whatman<sup>TM</sup>, GE Healthcare Europe, Germany). The control line was then printed in the same way with a goat anti-mouse IgG antibody (Ab6708, Abcam) at  $0.5 \text{ mg.mL}^{-1}$ . The lines were spaced from each other by 4 mm. Afterwards, as described in S3.1, the membranes were treated to improve their conservation over time and reduce the appearance of non-specific signals during migration<sup>31</sup>, assembled, cut, and used within 3 weeks of manufacture. Note that multiplexing is achieved by spatially separating the three capture antibodies and not by using multicolored NPs.

Since the time of interaction between species is short in LFA and because cross-reactivity occurs, the order of test lines along the strip was chosen to achieve the highest sensitivity with the lowest non-specific signals, as discussed briefly in our previous article<sup>26</sup>.

#### *LFA procedure (dipstick format).*

The composition of the running solution can strongly affect LFA performances, partly because undesirable interfacial problems can occur. In particular, non-specific interactions with capture or detection antibodies, or steric hindrance on the NP or nitrocellulose membrane can modify the background signal on the membrane as well as the assay sensitivity<sup>31,32</sup>. Based on empirical observations, it is generally accepted that a relatively high salt concentration increases the reproducibility and sensitivity of the LFA by controlling the pH and ionic strength of the running solution, thus avoiding protein denaturation<sup>32,33</sup>. On the other hand, it is recognised that zwitterionic or non-ionic detergents, such as CHAPS or Tween 20 respectively, i) stabilise proteins (particularly membrane proteins), ii) can renature antibody epitopes, iii) allow the sample to flow through the strip, iv) elute antigens adsorbed non-specifically on the membrane and v) act as blocking agents to saturate free binding sites, alone or in combination with proteins (BSA, ovalbumin, casein, ...), thereby reducing background on the membrane<sup>32-34</sup>. The addition of sodium azide also protects buffers from microbial contamination<sup>33</sup>.

Since the most suitable composition of the running solution depends on the system under study (strip components, antigens, antibodies, and nanoparticles)<sup>33</sup>, the trial-and-error method was applied with Tris-HCl or potassium phosphate-based buffers containing azide, at pH 7.4 or 8, and in the presence of different concentrations of several additives such as NaCl, BSA, CHAPS and/or Tween 20. The highest sensitivity was obtained with the following running buffer: 0.1 % BSA, 0.5 % Tween 20, 0.01 % azide and 150 mM NaCl in a potassium phosphate buffer – 100 mM, pH 7.4.

NPs were diluted in the running buffer and mixed together to give a solution containing 250  $\mu$ M of vanadate ions of each NP type. To limit the aggregation between NP<sub>SEG</sub>, NP<sub>SEH</sub> and NP<sub>SEI</sub> because of non-specific interactions arising with the different detection antibodies, the dispersions were sonicated at 4°C (450 W Branson sonicator, 40 %, 20 s). This step has been shown to improve the assay sensitivity while limiting the detection antibodies degradation<sup>35</sup>. 85  $\mu$ L of toxins diluted in the running buffer were dispensed into the wells of a 96-well plate, in addition of 15  $\mu$ L of NPs (100  $\mu$ L per well in total). The toxin concentrations indicated in our work refer to the final concentrations in 100  $\mu$ L of sample (the nanoparticle concentration is constant while the concentrations of the three toxins vary independently). Then, the strips were immediately dipped for 25 min. Since the quantitative signal reading of the test line changes during the first 20 min after the end of the migration (data not shown), the strips were allowed to dry at room temperature for at least 30 min. A schematic representation of the global procedure is displayed in S3.2. Known mixtures of toxins used to build the multiparameter calibration surface and “unknown” mixtures (spiked samples) used as a proof of concept were prepared in different batches of running buffers to induce some variability in the sample matrix.

#### *Image collection and processing.*

To illuminate and image the strips, the camera of a smartphone (Samsung Galaxy S7) was coupled to an in-house portable reader (Figure 2a) and an application was coded to photograph the strips with fixed capture parameters (Figure 2b). The image analysis was then performed using Matlab. It should be noted that with such settings, non-specific signals may be observed on the test line of strips analyzed in the absence of toxin<sup>26</sup>. This would disqualify the assay in the case of a naked eye reading, as with commercial LFAs labeled with gold NPs. However, since a quantitative readout is possible here in the absence of analyte, this does not raise any issue.

Briefly, Regions Of Interest (ROIs) were first defined around the test and control lines (Figure 2c)<sup>36,37</sup>. Then, to obtain the raw signal, the pixel intensities were averaged along the direction of migration for the red channel, as displayed in Figure 2d-f (dotted lines). These raw data were convoluted with a normalized Gaussian to obtain a smoothed curve whose integral is kept constant, and the resulting profiles (empty circles) were fitted with Gaussians (plain lines) on top of the background (dotted grey lines). The signal on the test line depends on the degree of specific and non-specific binding, which is related to environmental parameters such as humidity and temperature, or technical parameters, such as excitation intensity fluctuations. To minimize these interferences and allow for reliable quantification, the final signals were defined as the ratio of the Gaussian amplitude of the test line (provided the standard deviations of the fitting Gaussians were sufficiently narrow) to the background. Otherwise, they were set to zero. In order to obtain a robust detection the comparison to a reference signal is mandatory. The test line signals are commonly normalized by the signals of the control line. However, in the extended concentration range explored in this study, the control line may be saturated, thus preventing any accurate correction, and justifying the use of the background signal as a normalizing reference. See our previous work<sup>26</sup> as well as the supplementary information S4 for more details about the entire procedure.

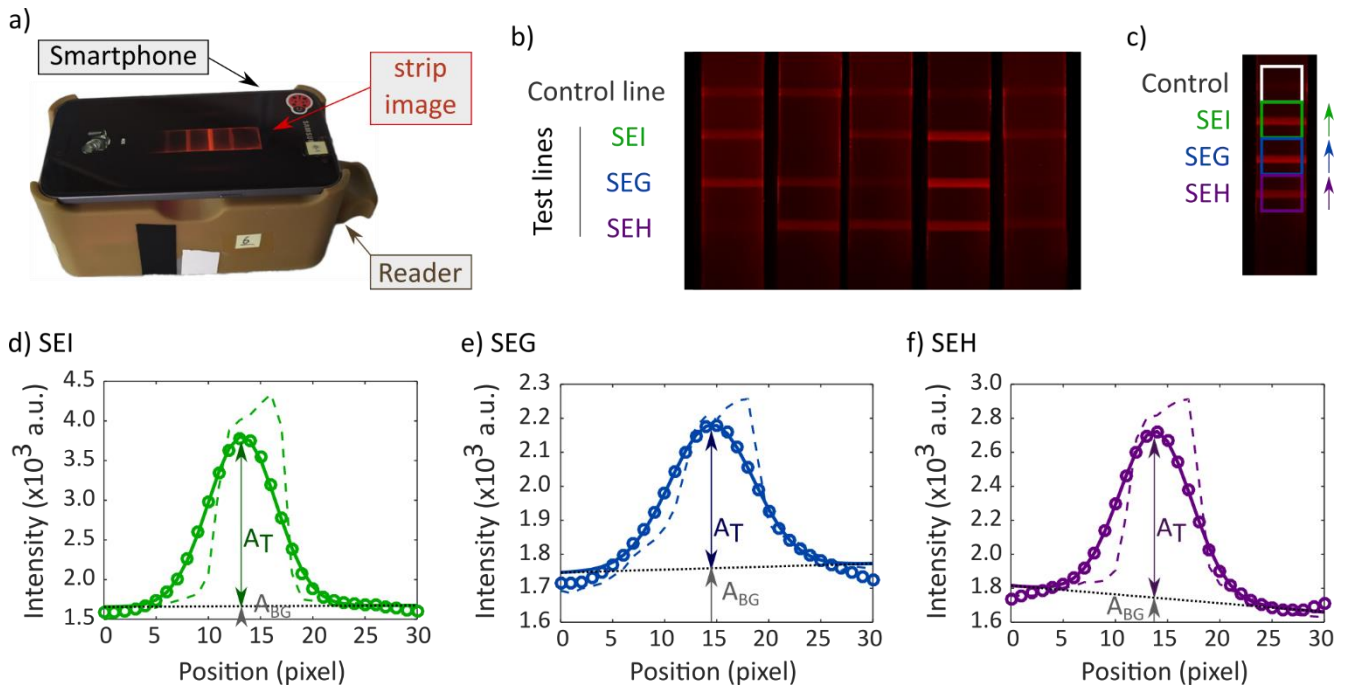


Figure 2: a) Smartphone coupled to the portable reader for LFA image capture. b) Example of LFA strips labeled with our luminescent nanoparticles for multiplexed detection of the three toxins. The triplets of SEG, SEH, and SEI concentrations, in  $\text{pg.mL}^{-1}$ , are {100 25 250}, {5 500 500}, {25 500 100}, {500 1000 500}, and {50 500 2.5}, respectively. c) Illustration of the position of Regions Of Interest (ROIs) around the control and test lines. d-f) Quantitative analysis of LFA strips shown in c) for the toxins SEI (d), SEG (e) and SEH (f) - The raw data (dotted lines) are the signals from the pixels within the ROI, averaged over the strip width and plotted as a function of position along the migration direction. The raw data are then convoluted by a Gaussian function and these convoluted data (empty circles) as well as the background are fitted by a Gaussian function and are displayed as a plain line and a grey dotted line respectively.  $A_T$  and  $A_{BG}$  represent their amplitudes.

#### Multi-gain detection for extended detection range.

In order to obtain a quantitative analysis over the widest possible concentration range, images were taken for different toxin concentrations with different values of camera gain. First, the camera sensor (Sony Exmor IMX1260) was characterized to determine its linear regime. In a second step, reference strips were imaged in order to determine the gain  $Gain_1$  allowing to remain in the linear detection regime, even at high concentration, while having the best signal-to-noise ratio. In parallel, we determined the gain  $Gain_2$  ( $Gain_2 > Gain_1$ ) allowing to detect the lowest concentrations and thus improve the assay sensitivity. Since the measurements relies on the ratiometric detection of band intensity, we expect to obtain gain-independent results and consequently perform efficient detection at optimal gain ( $Gain_2$  or  $Gain_1$ ), chosen only on an intensity criterion, without any prior knowledge of the sample. This was verified at intermediate concentrations, for which both gain values can be efficiently used and provided the same quantitative result, regardless of the gain. This innovative multi-gain imaging method therefore extends the range of quantifiable concentrations for both low and high concentrations, as displayed in S5.

#### Sensitivity estimation.

Different possible definitions of the LOB in the case of a multiplexed assay are given below, while their meaning is discussed in the paragraph “xLFA PERFORMANCES”.

1. Extension of the LOB defined for simplex assays:  $LOB_x = Zero_{\text{triple}} + 1.645 SD_{0,\text{triple}}$ , where  $Zero_{\text{triple}}$  and  $SD_{0,\text{triple}}$  are the mean signal and standard deviation of triple blank samples (*i.e.* of samples containing none of any of the three toxins).
2. Asymmetric LOB:  $LOB_{\text{asym}} = Zero_{\text{asym}} + 1.645 SD_{0,\text{asym}}$ , where  $Zero_{\text{asym}}$  and  $SD_{0,\text{asym}}$  are the mean signal and standard deviation of the blanks performed in the absence of the analyte of interest but in the presence of all the other targeted analytes at the maximum concentrations of the concentration range accessible for the assay. In our work, we can estimate the  $LOB_{\text{asym}}$  of the SEG, SEH, and SEI toxins respectively from {0 1000 500}, {500 0 500}, and {500 1000 0} pg.mL<sup>-1</sup> concentration triplets of SEG, SEH, and SEI.
3. Cross-reactive LOB:  $LOB_{\text{CR}} = Zero_{\text{CR}} + 1.645 SD_{0,\text{CR}}$  where  $Zero_{\text{CR}}$  and  $SD_{0,\text{CR}}$  are the mean signal and standard deviation of “single blanks”. In practice, we studied 30 single zeros {0, y, z} for the toxin X with y and z evenly distributed over the entire concentration range accessible in our test for the toxins Y and Z.

## Results and discussion

### DETERMINATION OF THE CONCENTRATION SPACE

To experimentally define the appropriate concentration range for each toxin (SEG, SEH, and SEI), strips are run with samples containing a single toxin over a wide concentration range and are analyzed quantitatively, as shown in S6. The appropriate concentration ranges for the evaluation of the multiplexed LFA (xLFA) and for the construction of the multiparameter surface are then chosen based on the following considerations. We mean to evenly distribute 10 concentrations across the linear range of the camera's optical response (in order to have non-saturated signals and be able to accurately quantify them). In the mean time, we want to test i) negative samples and ii) a few concentrations below the limit of blank (LOB) and above the limit of detection (LOD), for simplex samples run on multiplexed strips. For simplex assays, the LOB sets the concentration below which a sample without analyte has a 90% chance of being truly negative. It is defined as follows:  $LOB = Zero + 1.645 SD_0$  where  $Zero$  and  $SD_0$  are the mean signal and standard deviation of the blanks (*i.e.* samples without analyte), respectively<sup>38</sup>. The signal value corresponding to the LOD, defined by  $LOD = Zero + 3 SD_0$ , sets the concentration above which a sample has 99.7% chances of being truly positive<sup>38</sup>. Based on these considerations, the selected ranges are 1 - 500, 2.5 - 1000 and 1 - 500 pg.mL<sup>-1</sup> for SEG, SHE, and SEI, respectively, and these ranges define what we call the “3D concentration space”.

### RESPONSES IN MULTIPLEX TESTS

We first run control samples with 10 different concentrations for each of the toxins (including zero). We thus explore a subset of the concentration space containing 1 000 triplets (by retaining 100 of them) to estimate the raw performances of multiplexed tests in a large concentration range. These concentration triplets, noted {x,y,z}, are defined as follows. For a given toxin X, each of the 10 concentrations x is tested 10 times. For these 10 solutions, y and z vary independently through the 10 concentration values associated with them (see S7 for the list of 100 triplets). The multiplexed LFAs are then performed for the

100 concentration triplets, in independent triplicates (*i.e.* performed on three different days), and the strips are imaged (see S8) and analyzed as described in the M&M section.

The quantified signal for each toxin is then plotted as a function of the said toxin for SEG, SEH and SEI, as shown in Figure 3a-c. For a given toxin and concentration, the dispersion of different experimental points is both due to the variability between the replica and to the presence of different concentrations of the two other targets therefore inducing cross-reactivity. These signal points are indeed not only associated with unique replicates but with triplets of concentrations  $\{x,y,z\}$  with constant  $x$  and variable  $\{y,z\}$ . Our results thus demonstrate that it is not possible to quantitatively analyze multiplexed samples using calibration curves built with a single toxin present in solution, because of cross-reactivity, and that a new analytical method is therefore required to circumvent this drawback.

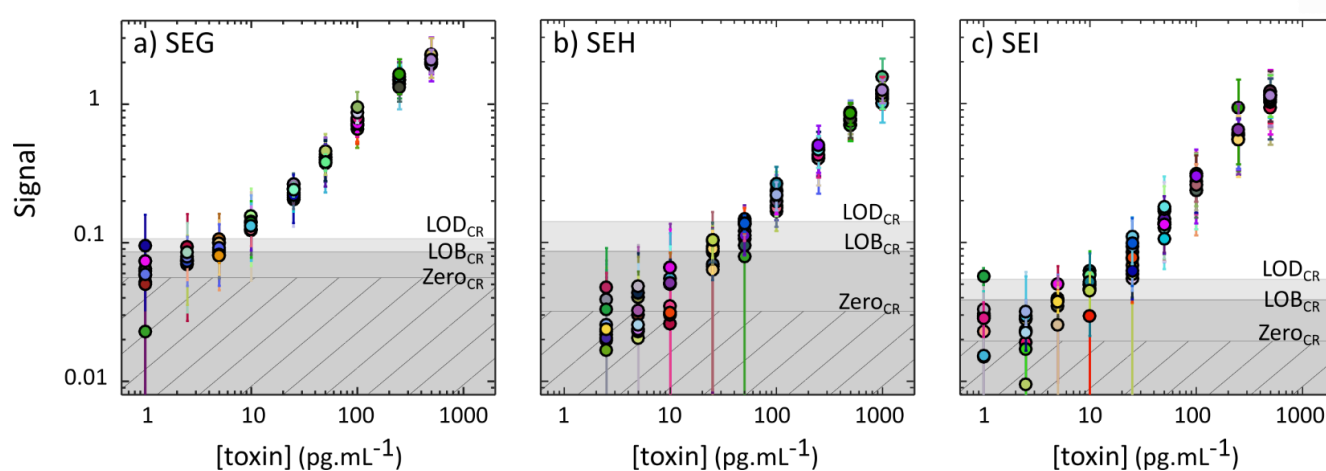


Figure 3: Signals as a function of the concentration for the 100 triplets of concentrations. Data are displayed separately for the toxins SEG (a), SEH (b), and SEI (c) to allow a better visualization of the results. The error bars correspond to the standard deviation of the three replicates performed for each triplet. Each triplet being associated with a unique color, points exhibiting the same color in both concentration and signal spaces correspond to the same point, *i.e.* to the same mixture of toxins. The “cross-reactive” Zero, LOB and LOD, respectively named Zero<sub>CR</sub>, LOB<sub>CR</sub> and LOD<sub>CR</sub>, take into account the cross-talk of the system, and are defined in the section M&M.

#### xLFA PERFORMANCES

On the basis of multiplexed detection, we estimate in the following the minimum detectable concentration for each toxin in the mixture. To do this, one might first think of extrapolating the definition introduced above for simplex detection. However, these LOBs, called “LOBx” and summarized in Table 1) do not take into account cross-reactivity and are therefore underestimated.

Another approach that considers cross-reactivity is based on the “Guidance document on multiplex real-time PCR methods” published in 2021 by the European Commission<sup>11</sup>. It is suggested that the ability to detect small amounts of each analyte of interest should be assessed in the presence of high amounts of the other target analytes, leading to the definition of an asymmetric LOB (LOB<sub>asym</sub>). However, the LOB of the analyte of interest probably increases when the concentrations of the other target analytes also increase. The LOB<sub>asym</sub> is therefore overestimated and provides an underestimate of the true sensitivity.

In the context of a multiplexed test with three target analytes, an actual LOB for a single analyte would no longer be a single concentration value but a 2D surface, due to the presence of cross-reactivity. In order to consider this phenomenon over the entire concentration space, we define a new practical sensitivity indicator, called cross-reactive LOB ( $LOB_{CR}$ ), as the typical minimal signal that can be detected with our device. In practice, blank samples consist of different doublets of concentrations, with a single toxin concentration set to zero. This allows to take into account all cross-reactivity information contained in the system under study. Furthermore, as illustrated with the SEH toxin at 25  $\text{pg}\cdot\text{mL}^{-1}$  (Figure 3b), the  $LOB_{CR}$  cannot be given in terms of concentrations because different  $\{x\ 25\ z\}$   $\text{pg}\cdot\text{mL}^{-1}$  triplets of the SEG, SEH, and SEI toxins, respectively, show that the minimal detectable concentration [SEH] depends on the values of  $\{x\ z\}$ . Given these considerations,  $LOB_{CR}$  are determined in terms of signal values at 0.08, 0.08, and 0.04 for SEG, SEH, and SEI, respectively (Figure 3 and Table 1).

toxin	$LOB_x$ ( $\text{pg}/\text{mL}$ )	$LOD_x$ ( $\text{pg}/\text{mL}$ )	$LOB_{CR}$	$LOD_{CR}$	$LOB_{app}$ ( $\text{pg}/\text{mL}$ )	$LOD_{app}$ ( $\text{pg}/\text{mL}$ )
SEG	2	5	0.08	0.11	3	6
SEH	6	37	0.08	0.13	27	48
SEI	5	14	0.04	0.05	6	11

Table 1: LOB and LOD values in terms of signal or concentration according to the different definitions explained in the text. Note that i) the  $LOB_x$  and  $LOD_x$  are issued from our data shown in S6 and ii)  $LOB_{CR}$  are without unit since they are given in terms of signal values, as discussed in the text.

To estimate the typical performance of our assay and compare it to that described in the literature, the 10 results obtained for the  $\{x\ y\ z\}$  concentration triplets with fixed  $x$  and variable  $y$  and  $z$  were averaged (see S9). This convention allows us to determine an apparent detection limit  $LOB_{app}$  in terms of concentration, averaging out the effects of cross-reactivity. We obtained  $LOB_{app} = 3, 27, \text{ and } 6\ \text{pg}\cdot\text{mL}^{-1}$  for SEG, SEH, and SEI toxins, respectively (Table 1). As expected, these values are slightly higher than those obtained in S6 from triple zeros ( $LOB_x$ ).

Finally, these results show that we have developed a multiplexed LFA allowing the detection of three SEs toxins over 2 orders of magnitude in concentration for each toxin and without saturation of the measured signal, which is important for medical diagnosis. Indeed, in a biological sample, different proteins can be present at concentrations spanning several decades<sup>4</sup>. It is therefore advantageous to have an assay that allows quantitative analysis over a wide concentration range in order to measure simultaneously, and in the same sample, low and high abundance proteins<sup>7</sup>. Moreover, our assay is approximately 100 times more sensitive than what is described in the literature for multiplexed detection of SEs toxins by LFA compatible with in-field use<sup>39</sup>. Our assay is also 5 to 40 times more sensitive than Vidas SET 2 and RidaScreen SET Total, the two commercially available ELISA kits authorized by European legislation for the detection of SEs in food matrices<sup>40,41</sup>. This is due to the use of the high affinity antibodies we have developed<sup>27</sup>, and our more sensitivity approach based on ultra-bright rare earth doped nanoparticle imaging<sup>26</sup> combined to our novel analytical method.

#### ESTABLISHMENT AND PRINCIPLE OF USE OF THE MULTIPARAMETER SURFACE

To ensure that cross-reactivity is no longer an obstacle to quantification in multiplexed LFA, we produce a single so-called multiparameter calibration surface. The 100 triplets of concentrations studied before, and the 100 corresponding triplets of signals are now used as calibration points (Figures 4a and 4c respectively). In order to retrieve the undetermined concentrations of toxins

in an unknown sample, the signal space was tessellated by a 3D-Delaunay triangulation in tetrahedrons, where each vertex corresponds to a signal triplet associated with a sample, *i.e.* with a concentration triplet (Figure 4 c-d). To ensure an unambiguous determination of the concentrations in the unknown toxin mixture, we first check that each triplet of signals in the explored ranges corresponds to a unique triplet of concentration (see S10 for more details). With this verification, we can claim that we have built a multiparameter calibration surface for xLFA by measuring the signal triplets associated with the 100 concentration triplets. Note that in the case of quantitative multiplexed immunoassays, the calibration surface, *i.e.* the way of determining the concentration from the measure of a given signal, is not a usual 2D curve but a function relating two 3D spaces.

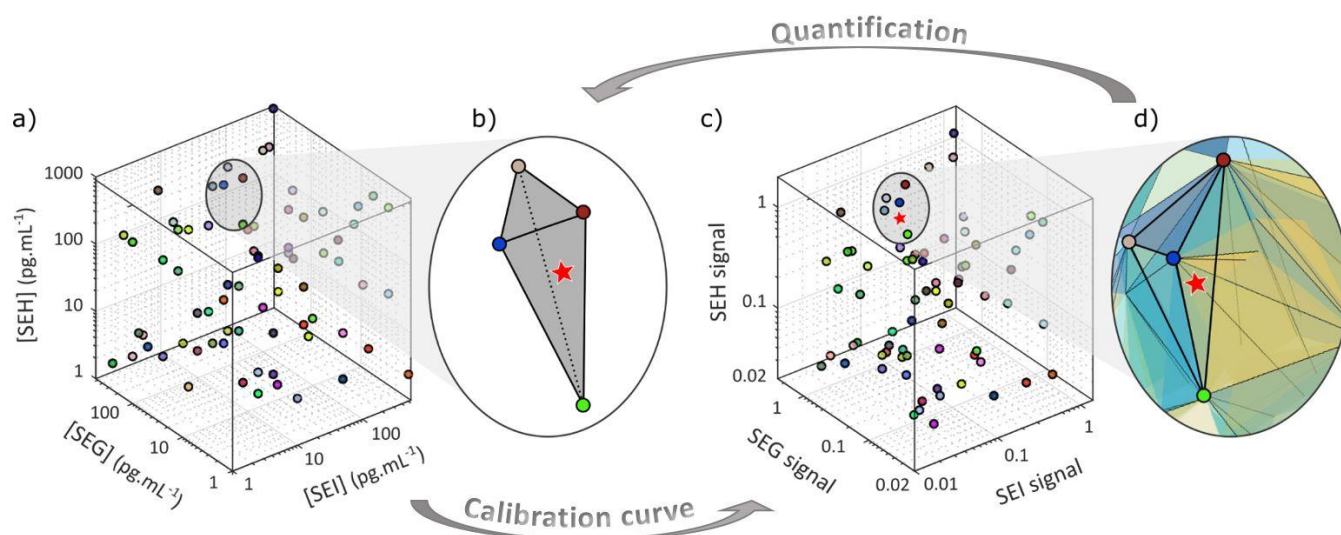


Figure 4: a,c) Distribution of the 100 triplets selected for the construction of the multiparameter calibration surface in the 3D space of concentrations (a) and of their corresponding quantified signals in the 3D space of signals (c). The triplets are associated to a unique color, meaning that a point which has the same color in Figure 3 or in Figure 4 corresponds to the same triplet of concentrations. b,d) Example of the determination of the triplet of concentrations for an unknown sample (represented here by a red star). The 3D space of signals is paved by tetrahedrons defined with a Delaunay tessellation. After migration across the strip, the signals on the test lines are quantified, leading to the determination of the tetrahedron containing the resulting triplet of signals (d). The corresponding tetrahedron is then selected in the 3D concentration space (b), enabling the determination of the triplet of concentrations associated to the unknown sample.

Since the transformation between the concentration space and the signal space is bijective, the concentration of toxins could be determined by performing the following protocol: i) run the xLFA for the unknown sample, ii) quantify the signal triplet associated with the strip image, which yields its cartesian coordinates in the signal space, iii) find the tetrahedron in the signal space that contains our triplet (Figure 4d), iii) determine its barycentric coordinates in the reference frame defined by the axes of the tetrahedron, iv) use these barycentric coordinates to position the sample in the associated tetrahedron located in concentration space (red star, Figure 4b), v) read its cartesian coordinates in the concentration space, which corresponds to the concentration triplet of the unknown sample under investigation. With this innovative method of analysis, cross-reactivity is no longer a drawback that hinders quantification in multiplexed systems, even in the configuration in which this phenomenon has not been limited by the use of multicolor probes.

## ENTEROTOXIN MULTI-TITRATION

We then demonstrate the feasibility to efficiently titrate the concentrations of enterotoxin mixtures (SEG, SEH, SEI) of *a priori* unknown compositions through our analytical method (see *supra*): 11 samples are thus spiked with toxin triplets whose concentrations were not previously used to construct the multiparameter calibration surface (Figure 5a). The tests are performed with a fresh batch of buffer (M&M) in order to introduce some variability and to mimic the fact that with real samples (*e.g.* with river water), the sample matrix will be different from the buffer used to perform the calibration performed upstream. The LFA strips are then imaged (Figure 5b) and analyzed with the same methodology used to obtain the calibration points (M&M). Finally, the concentration triplets are determined using the multiparameter calibration surface, as discussed above. The results are then plotted on the same graph as the calibration surface which demonstrates the presence of an offset between the two curves for each of the three toxins (see S11). We attribute this offset to the fact that the unknown samples and the solutions used to construct the multiparameter calibration surface were prepared with different batches of running buffer<sup>42</sup>. The offset is easily corrected for each toxin by running a strip with a defined triplet of concentrations in addition to the “unknown” mixtures, as explained in S11 and displayed in Figure 5d-f. Nevertheless, one should verify that our correction of the offset is still valid for samples run in complex matrices.

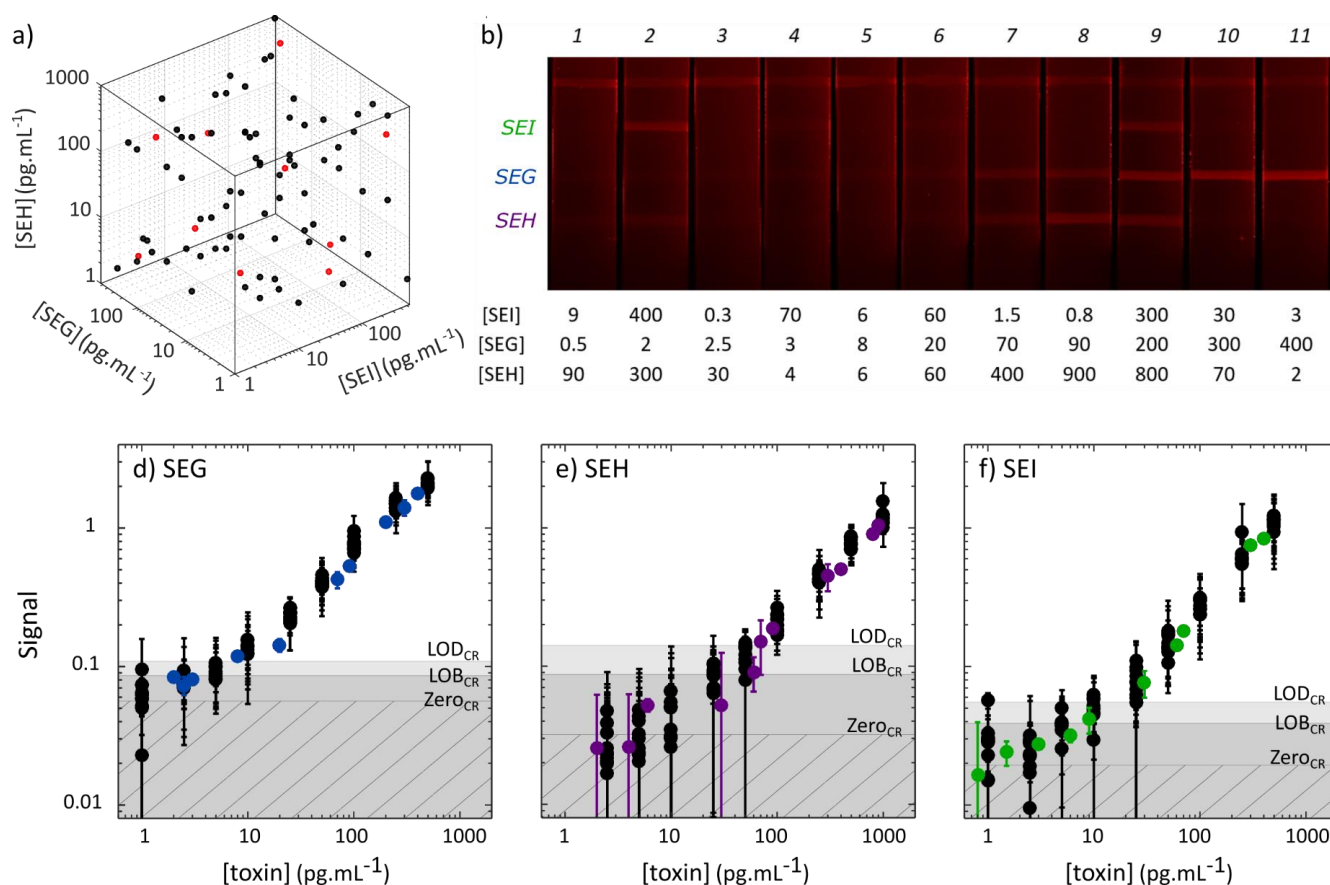


Figure 5: a) Distribution in the 3D concentration space of the 11 triplets of spiked concentrations (*i.e.* the 11 “unknown” samples) shown as red circles. The black circles indicate the 100 samples used for the calibration. b) Images of the corresponding strips after migration (concentrations are in pg.mL<sup>-1</sup>). d-f) Signals obtained for the unknown samples as a function of the spiked concentrations, after correction for the offset (see text). Data are displayed separately in blue, purple and green for the toxins SEG (d), SEH (e), and SEI (f) respectively, to allow a better visualization of the results together with the data from the calibration samples in black.

We then compare the actual concentration with its estimation through our analytical procedure to deduce its reliability (Figure 6). The precision of an assay is usually estimated *via* the coefficient of variation (CV), defined as the ratio between the standard deviation (SD) and the mean of measurements carried out in replicates, at a given concentration<sup>43,44</sup>. A CV value below 15 % (respectively 20 %) is required for clinical applications according to the EMA ref (respectively FDA ref ) guidance, while a CV lower than 20 to 30 % is considered adequate for the majority of other applications<sup>43,44</sup>. In multiplexed assays, an actual CV for a single analyte would no longer be a single value but a 2D surface, as discussed above for the LOB. To take into account the phenomenon of cross-reactivity over the entire concentration space, we define a new practical precision index, called cross-reactive CV ( $CV_{CR}$ ), corresponding to the mean of the CV for each concentrations of the toxin of interest in the presence of different cocktails of the other toxins.  $CV_{CR}$  is calculated as follow, where  $[spiked]_n$  and  $[estimated]_n$  are respectively the spiked and estimated concentrations of the considered toxin of the sample n.

$$CV_{CR} = mean(CV_n) \text{ with } CV_n = 100 * \frac{SD([spiked]_n, [estimated]_n)}{mean([spiked]_n, [estimated]_n)}$$

For samples with signals above the  $LOB_{CR}$ , we obtained an average  $CV_{CR}$  of 20%, and more than 80% of the concentrations are determined with a CV of less than 30%. Recovery rates, classically defined by  $recovery = 100 * \frac{[estimated]_n - [spiked]_n}{[spiked]_n}$  are found at  $100\% \pm 24\%$ , which is within the recommended range for simplex assays ( $100\% \pm 20/30\%$ )<sup>43,44</sup>, and which is therefore excellent for a multiplexed quantitative test in the presence of cross-reactivity, demonstrating the robustness and accuracy of our strip analysis method and of the offset correction.

Finally, our work demonstrates that we are able to accurately quantify the concentrations of three toxins in unknown samples, despite the presence of cross-reactivity, and with good precision, for nearly two decades of concentrations, and for typical concentrations as low as the LOB ( $\sim 3 \text{ pg.mL}^{-1}$ ). These results bode well for the development of ultra-sensitive quantitative tests, especially since improvements in analytical sensitivity could be obtained by increasing the effective affinity and selectivity of the detection antibodies, by finely tuning the nanoparticle size or the Ab-to-NP ratio, or by using multicolor NPs<sup>45-47</sup>.

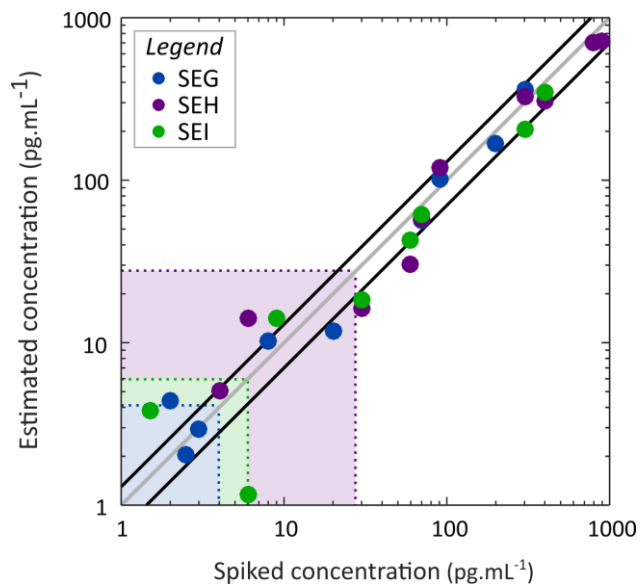


Figure 6: Estimated concentrations as a function of the spiked concentration for the « unknown » samples. Data for the SEG, SEH, and SEI toxins are respectively shown in blue, purple and green. The corresponding squares define areas where spiked and measured concentrations are below the respective  $LOB_{CR}$ . The grey diagonal line corresponds to a 100 % recovery and the black lines delimit a 30 % CV.

		Mean CV	Samples with CV < 30 %
Offset correction	without	36 %	25 %
	with	20 %	80 %

Table 2: Accuracy of the recovery in spiked samples without and with the correction of the offset.

## Conclusion

Here, we set out an original analytical methodology, based on the construction of a multiparameter calibration surface to perform multiplexed quantitative detection in the presence of cross-reactivity. By coupling the tools developed in our previous work (probe, antibodies and reader)<sup>26</sup> to this new technique, we were able to perform multi-titration on unknown protein mixtures with high accuracy ( $CV_{CR} < 30\%$ , recovery = 20 %) and sensitivity (LODs values as low as few  $\text{pg.mL}^{-1}$ ) while preserving the features of the LFA without hindering its deployment on site.

In complex clinical scenarios, such as Covid-19, inflammatory or neurodegenerative diseases, and cancer, variations in the levels and ratios of several biomarkers in the  $\text{pg.mL}^{-1}$  range give insight on the presence, severity and progression of the corresponding illnesses<sup>1,4,7,48</sup>. The detection of a single biomarker may be insufficient for clinical diagnosis or assessment of disease progression. In addition, Point of Care (POC) assays usually display LOD concentrations at the  $\text{ng.mL}^{-1}$  level and detect a single analyte, which limits their use for the detection of many biomarkers. In this context, our methodology paves the way for efficient diagnosis procedures since it allows for a quantitative, sensitive ( $\text{pg.mL}^{-1}$ ), and multiplexed POC assay, but for a limited number of target analytes detected simultaneously.

To perform a quantitative multiplexed test on a large number of targets, the format of our LFA needs to be adapted. On the one hand, we could print several dozen test spots rather than printing test lines, thus performing Lateral Flow Microarrays (LFM)<sup>2,4</sup>, but *de facto* increasing the cross-reactivity<sup>8</sup>. On the other hand, we could implement a multicolor detection of different targets within a single test area but this methodology is limited by the restricted number of colors accessible without spectral overlap and by the fact that too high a density of antibodies decreases the assay sensitivity<sup>46,47,49</sup>. However, these two approaches are not mutually exclusive and large-scale multiplexing could benefit from their combination with the development of multicolor LFMs.

Metal nanoparticles have been successfully used for multicolor multiplexing<sup>22,25</sup>. However, they are prone to aggregation, which alters their optical properties and the quantitative outcome of the assay. In addition, these and other colored probes such as dye-doped latex nanoparticles are not very sensitive<sup>6,22,25</sup>, unlike luminescent probes such as quantum dots<sup>17,18,24</sup>, up-conversion particles<sup>20,21</sup>, polymer dots<sup>19</sup>, or persistent luminescent nanophosphors<sup>23</sup>. However, the difficulties associated with the synthesis of particles of different colors and the possible need to multiply the sources of excitation, though restrict the choice of NPs suitable for producing a multicolor LFM whose ease of implementation and cost would remain comparable to that of simplex LFAs.

In this context, our probes are an interesting basis for the development of a multicolor LFMs. Replacement of the europium ions doping our  $\text{YVO}_4:\text{Eu}$  nanoparticles with other lanthanide ions (Ln) is straightforward and their excitation in the UV is feasible *via* the  $\text{YVO}_4$  matrix<sup>50,51</sup>, using for instance our compact and inexpensive in-house reader. The combination of our analytical method, our reader and various  $\text{YVO}_4:\text{Ln}$  probes thus opens the way to the development of a new generation of assays, that are *a priori* suitable for large-scale multiplexing, allowing simultaneous, quantitative and ultra-sensitive detection of many analytes despite the presence of cross-reactivity. In addition, it could be easily adapted to the detection of protein biomarkers to provide a

resource for immediate clinical decision-making, and to develop better personalised healthcare, faster but just as sensitive than ELISA tests.

## Author contributions

All authors contributed to the writing of the manuscript and have given approval to the final version. F. Mousseau designed/performed the experiments and wrote the Matlab script, C. Féraudet Tarris and S. Simon provided the antibodies and toxins, T. Gacoin provided and characterized the lanthanide-based nanoparticles, A. Alexandrou designed experiments, and C. I. Bouzigues designed experiments and wrote the Matlab script.

## Conflicts of interest

There are no conflicts of interest to declare.

## Acknowledgements

We are grateful to Rabei Mohammadi (Ecole Polytechnique, Laboratory PMC, France) for the synthesis of the europium-doped nanoparticles, to Jean-Marc Sintès and Xavier Solinas (Ecole Polytechnique, Laboratory LOB, France) for their contribution to the reader development, and to Timma Mohammed-Ali for fruitful discussions on the dual gain imaging method. This project was funded through the Agence Innovation Défense (AID) grant SPIDERMAP and the Centre Interdisciplinaire d'Etude pour la Défense et la Sécurité (CIEDS) grant DAVID. For the TEM experiments shown in SI, the present work has benefited from the Imagerie–Gif core facility supported by l'Agence Nationale de la Recherche (ANR-11-EQPX-0029/Morphoscope, ANR-10-INBS-04/FranceBioImaging, ANR-11-IDEX-0003-02/Saclay Plant Sciences).

## Bibliography

1. Gil Rosa, B. *et al.* Multiplexed immunosensors for point-of-care diagnostic applications. *Biosensors and Bioelectronics* **203**, 114050 (2022).
2. Anfossi, L., Di Nardo, F., Cavalera, S., Giovannoli, C. & Baggiani, C. Multiplex Lateral Flow Immunoassay: An Overview of Strategies towards High-throughput Point-of-Need Testing. *Biosensors* **9**, 2 (2018).
3. Kosack, C. S., Page, A.-L. & Klatser, P. R. A guide to aid the selection of diagnostic tests. *Bulletin of the World Health Organization* **95**, 639–645 (2017).
4. Sena-Torralba, A., Álvarez-Diduk, R., Parolo, C., Piper, A. & Merkoçi, A. Toward Next Generation Lateral Flow Assays: Integration of Nanomaterials. *Chem. Rev.* **122**, 14881–14910 (2022).

5. Nguyen, V.-T., Song, S., Park, S. & Joo, C. Recent advances in high-sensitivity detection methods for paper-based lateral-flow assay. *Biosensors and Bioelectronics* **152**, 112015 (2020).
6. Lee, S., Mehta, S. & Erickson, D. Two-Color Lateral Flow Assay for Multiplex Detection of Causative Agents Behind Acute Febrile Illnesses. *Anal. Chem.* **88**, 8359–8363 (2016).
7. Cohen, L. & Walt, D. R. Highly Sensitive and Multiplexed Protein Measurements. *Chem. Rev.* **119**, 293–321 (2019).
8. Juncker, D., Bergeron, S., Laforte, V. & Li, H. Cross-reactivity in antibody microarrays and multiplexed sandwich assays: shedding light on the dark side of multiplexing. *Current Opinion in Chemical Biology* **18**, 29–37 (2014).
9. Mohd Hanafiah, K. *et al.* Development of Multiplexed Infectious Disease Lateral Flow Assays: Challenges and Opportunities. *Diagnostics* **7**, 51 (2017).
10. Van Gool, A. *et al.* Analytical techniques for multiplex analysis of protein biomarkers. *Expert Review of Proteomics* **17**, 257–273 (2020).
11. European Commission. Joint Research Centre. *Guidance document on multiplex real-time PCR methods*. (Publications Office, 2021).
12. Slaastad, H. *et al.* Multiplexed immuno-precipitation with 1725 commercially available antibodies to cellular proteins. *Proteomics* **11**, 4578–4582 (2011).
13. Li, H., Bergeron, S. & Juncker, D. Microarray-to-Microarray Transfer of Reagents by Snapping of Two Chips for Cross-Reactivity-Free Multiplex Immunoassays. *Anal. Chem.* **84**, 4776–4783 (2012).
14. Dagher, M. *et al.* *nELISA: A high-throughput, high-plex platform enables quantitative profiling of the secretome*. <http://biorxiv.org/lookup/doi/10.1101/2023.04.17.535914> (2023) doi:10.1101/2023.04.17.535914.
15. Whiteaker, J. R. *et al.* Evaluation of Large Scale Quantitative Proteomic Assay Development Using Peptide Affinity-based Mass Spectrometry. *Molecular & Cellular Proteomics* **10**, M110.005645 (2011).
16. Kelley, E. J. *et al.* Virome-wide detection of natural infection events and the associated antibody dynamics using longitudinal highly-multiplexed serology. *Nat Commun* **14**, 1783 (2023).
17. Taranova, N. A., Berlina, A. N., Zherdev, A. V. & Dzantiev, B. B. ‘Traffic light’ immunochromatographic test based on multicolor quantum dots for the simultaneous detection of several antibiotics in milk. *Biosensors and Bioelectronics* **63**, 255–261 (2015).
18. Foubert, A. *et al.* Development of a Rainbow Lateral Flow Immunoassay for the Simultaneous Detection of Four Mycotoxins. *J. Agric. Food Chem.* **65**, 7121–7130 (2017).
19. Fang, C.-C. *et al.* Multiplexed Detection of Tumor Markers with Multicolor Polymer Dot-Based Immunochromatography Test Strip. *Anal. Chem.* **90**, 2134–2140 (2018).
20. He, H. *et al.* Quantitative Lateral Flow Strip Sensor Using Highly Doped Upconversion Nanoparticles. *Anal. Chem.* **90**, 12356–12360 (2018).
21. Jin, B. *et al.* Lateral flow aptamer assay integrated smartphone-based portable device for simultaneous detection of multiple targets using upconversion nanoparticles. *Sensors and Actuators B: Chemical* **276**, 48–56 (2018).
22. Di Nardo, F. *et al.* Colour-encoded lateral flow immunoassay for the simultaneous detection of aflatoxin B1 and type-B fumonisins in a single Test line. *Talanta* **192**, 288–294 (2019).
23. Danthararyana, A. N. *et al.* A multicolor multiplex lateral flow assay for high-sensitivity analyte detection using persistent luminescent nanophosphors. *Anal. Methods* **12**, 272–280 (2020).
24. Zou, J. *et al.* Rapid and simultaneous detection of heart-type fatty acid binding protein and cardiac troponin using a lateral flow assay based on metal organic framework@CdTe nanoparticles. *Nanoscale* **13**, 7844–7850 (2021).

25. Zhang, Y., Yu, Y. & Ying, J. Y. Multi-Color Au/Ag Nanoparticles for Multiplexed Lateral Flow Assay Based on Spatial Separation and Color Co-Localization. *Adv Funct Materials* **32**, 2109553 (2022).
26. Mousseau, F. *et al.* Luminescent lanthanide nanoparticle-based imaging enables ultra-sensitive, quantitative and multiplexed *in vitro* lateral flow immunoassays. *Nanoscale* **13**, 14814–14824 (2021).
27. Féraudet Tarisse, C. *et al.* Highly sensitive and specific detection of staphylococcal enterotoxins SEA, SEG, SEH and SEI by immunoassay. *Toxins* **13**, 130 (2021).
28. Wu, S. *et al.* A Review of the Methods for Detection of Staphylococcus aureus Enterotoxins. *Toxins* **8**, 176 (2016).
29. Lefebvre, D. *et al.* Quantitative Determination of *Staphylococcus aureus* Enterotoxins Types A to I and Variants in Dairy Food Products by Multiplex Immuno-LC-MS/MS. *J. Agric. Food Chem.* **69**, 2603–2610 (2021).
30. Neouze, M.-A. *et al.* Toward a Chemical Control of Colloidal YVO<sub>4</sub> Nanoparticles Microstructure. *Langmuir* **36**, 9124–9131 (2020).
31. de Puig, H., Bosch, I., Gehrke, L. & Hamad-Schifferli, K. Challenges of the Nano–Bio Interface in Lateral Flow and Dipstick Immunoassays. *Trends in Biotechnology* **35**, 1169–1180 (2017).
32. Javani, A., Javadi-Zarnaghi, F. & Rasaei, M. J. Development of a colorimetric nucleic acid-based lateral flow assay with non-biotinylated capture DNA. *Appl Biol Chem* **60**, 637–645 (2017).
33. Parolo, C. *et al.* Tutorial: design and fabrication of nanoparticle-based lateral-flow immunoassays. *Nat Protoc* **15**, 3788–3816 (2020).
34. Zampieri, S. *et al.* The use of Tween 20 in immunoblotting assays for the detection of autoantibodies in connective tissue diseases. *Journal of Immunological Methods* **239**, 1–11 (2000).
35. Dias, J. T., Lama, L., Gantelius, J. & Andersson-Svahn, H. Minimizing antibody cross-reactivity in multiplex detection of biomarkers in paper-based point-of-care assays. *Nanoscale* **8**, 8195–8201 (2016).
36. Scherr, T. F., Gupta, S., Wright, D. W. & Haselton, F. R. Mobile phone imaging and cloud-based analysis for standardized malaria detection and reporting. *Sci Rep* **6**, 28645 (2016).
37. Paterson, A. S. *et al.* A low-cost smartphone-based platform for highly sensitive point-of-care testing with persistent luminescent phosphors. *Lab Chip* **17**, 1051–1059 (2017).
38. Armbruster, D. A. & Pry, T. Limit of Blank, Limit of Detection and Limit of Quantitation. *Clin Biochem Rev* **29**, 4 (2008).
39. Wang, W. *et al.* Gold-Nanoparticle-Based Multiplexed Immunochromatographic Strip for Simultaneous Detection of Staphylococcal Enterotoxin A, B, C, D, and E. *Part. Part. Syst. Charact.* **33**, 388–395 (2016).
40. VIDAS® Staph enterotoxin II (SET2) - user instructions; bioMérieux SA, Marcy l’Etoile, France.
41. RIDASCREEN® SET A,B,C,D,E - user instructions; R-Biopharm AG, Darmstadt, Germany.
42. Helen Hsieh, Jeffrey Dantzler, & Bernhard Weigl. Analytical Tools to Improve Optimization Procedures for Lateral Flow Assays. *Diagnostics* **7**, 29 (2017).
43. Andreasson, U. *et al.* A Practical Guide to Immunoassay Method Validation. *Front. Neurol.* **6**, (2015).
44. Cox, K. L., Devanarayan, V., Kriauciunas, A., Montrose, C. & Sittampalam, S. Immunoassay Methods. *Book chapter of the Assay Guidance Manual* (2019).
45. Xu, H. *et al.* Gold-Nanoparticle-Decorated Silica Nanorods for Sensitive Visual Detection of Proteins. *Anal. Chem.* **86**, 7351–7359 (2014).
46. Byzova, N. A., Safenkova, I. V., Slutskaya, E. S., Zherdev, A. V. & Dzantiev, B. B. Less is More: A Comparison of Antibody–Gold Nanoparticle Conjugates of Different Ratios. *Bioconjugate Chem.* **28**, 2737–2746 (2017).

47. Malaspina, D. C., Longo, G. & Szleifer, I. Behavior of ligand binding assays with crowded surfaces: Molecular model of antigen capture by antibody-conjugated nanoparticles. *PLoS ONE* **12**, e0185518 (2017).
48. Tjendra, Y. *et al.* Predicting Disease Severity and Outcome in COVID-19 Patients: A Review of Multiple Biomarkers. *Archives of Pathology & Laboratory Medicine* **144**, 1465–1474 (2020).
49. Cowsill, B. J. *et al.* Interfacial Structure of Immobilized Antibodies and Perdeuterated HSA in Model Pregnancy Tests Measured with Neutron Reflectivity. *Langmuir* **30**, 5880–5887 (2014).
50. Riwotzki, K. & Haase, M. Wet-Chemical Synthesis of Doped Colloidal Nanoparticles:  $\text{YVO}_4:\text{Ln}$  (Ln = Eu, Sm, Dy). *J. Phys. Chem. B* **102**, 10129–10135 (1998).
51. Yang, L., Peng, S., Zhao, M. & Yu, L. New synthetic strategies for luminescent  $\text{YVO}_4:\text{Ln}^{3+}$  (Ln = Pr, Sm, Eu, Tb, Dy, Ho, Er) with mesoporous cell-like nanostructure. *Opt. Mater. Express* **8**, 3805 (2018).